Phyton-
International Journal of
Experimental Botany

Tech Science Press

http://doi.org/10.32604/phyton.2026.075718

ARTICLE

Metabolite Profiling and Skin Anti-Aging Potential of *Astragalus sarcocolla*: Antioxidant, Enzyme Inhibitory, and Computational Insights

Shaimaa R. Ahmed[1,*], Omnia M. Hendawy[2], Sumera Qasim[2], Hanan Khojah[3] and Ambreen Malik Uttra[4]

[1]Department of Pharmacognosy, College of Pharmacy, Jouf University, Sakaka, Aljouf, Saudi Arabia
[2]Department of Pharmacology, College of Pharmacy, Jouf University, Sakaka, Aljouf, Saudi Arabia
[3]Department of Pharmacognosy, College of Pharmacy, Nursing and Medical Sciences, Riyadh Elm University, Riyadh, Saudi Arabia
[4]Department of Pharmacology, College of Pharmacy, University of Sargodha, Sargodha, Pakistan
*Corresponding Author: Shaimaa R. Ahmed. Email: srmorsi@ju.edu.sa

Received: 06 November 2025; Accepted: 16 January 2026; Published: 28 February 2026

ABSTRACT: The study evaluated the skin anti-aging activity of *Astragalus sarcocolla* leaves extract (ASE) by assessing its antioxidant and inhibitory effect activity on matrix metalloproteinase (MMP), collagenase, elastase, hyaluronidase, and tyrosinase in relation to its chemical composition. Ultra Performance Liquid Chromatography-Mass Spectrometry (UPLC-MS) identified 27 metabolites (15 flavonoids, 8 phenolic acids and their derivatives, and 4 coumarins). ASE showed strong antioxidant capacity in DPPH (IC_{50} value of 26.05 μg/mL) and FRAP (2433 μM $FeSO_4$/g extract) assays. The extract inhibited MMP-1 and MMP-9 in a concentration-dependent manner and suppressed collagenase, elastase, hyaluronidase, and tyrosinase activities (IC_{50} = 35.038, 40.748, 61.389, and 30.980 μg/mL, respectively). A network pharmacology study was conducted to uncover the mechanisms responsible for skin anti-aging effects, and molecular docking further evaluated interactions of key metabolites with hub targets. Twenty-one bioactive metabolites, selected based on oral bioavailability and drug-likeness, highlighted cinnamic acid, acacetin, luteolin, kaempferol, and apigenin as key compounds. MMP-9, ESR1, PTGS-2, and EGFR were identified as main targets. Docking studies revealed that acacetin and apigenin have stronger binding affinities to MMP-9, PTGS-2, and EGFR than other constituents. These findings suggest that ASE may serve as a natural multi-target skin anti-aging remedy with potential cosmetic applications.

KEYWORDS: *Astragalus sarcocolla*; metabolite profiling; aging; metalloproteinase; network pharmacology

1 Introduction

Aging is a natural process that affects all living organisms. The skin is the body's main organ and plays a crucial role in social interactions. Skin aging has increasingly become a major concern in today's society. Aging is a multifaceted process that disturbs the skin through various structural, biochemical, and physiological changes. These changes occur in both the epidermis (outer layer) and dermis (deeper layer) of the skin [1]. Over time, collagen and elastin fibers in the dermis break down, leading to a loss of skin firmness and elasticity and the formation of fine lines and deeper wrinkles. In addition to these structural changes, aging also affects the skin's ability to retain moisture, causing dehydration and rough texture. Biochemically, the skin's renewal process slows, causing dead skin cells to accumulate on the surface, further contributing to a dull and dry appearance. Pigmentation changes, such as age spots, occur as melanin production becomes less regulated with age. These changes combine together to produce visible

signs of aging (sagging, fine lines, wrinkles, dryness, and uneven skin pigmentation) [2]. Skin aging is caused by two factors: intrinsic aging (chronological aging), i.e., degeneration of biological functions that occurs with time, and extrinsic aging (premature skin aging), which results from environmental factors like ultraviolet (UV) radiation, smoking, high temperatures, and air pollution [3]. Therefore, clinicians need to have a deep understanding of the physiology of skin aging in order to create a treatment plan that involves choosing anti-aging procedures aimed at specific mechanisms of skin aging, all while minimizing side effects.

A proper model is required to conduct an effective skin study. Through the years, *in vitro*, *in vivo*, and *in-silico* methodologies have developed as key tools in pharmaceutical and cosmetic testing. Nonetheless, there has been a growing concern about minimizing animal use in healthcare and cosmetic testing, which is consistent with the "3R" principles of replacement, reduction, and refinement. Since 1993, most countries have prohibited animal experiments in cosmetics production. European Union countries started implementing the limitations on animal experiments seriously in 2013. As a result, non-animal approaches, such as *in vitro* skin models, have become more widely developed and employed, gradually replacing traditional animal studies [4,5].

Matrix metalloproteinases (MMPs) are enzymes involved in the breaking down and remodeling of the extracellular matrix, particularly collagen and elastin, two proteins that support and preserve skin structure and elasticity. Each MMP has a distinct role in skin structure and appearance. MMPs are activated by UV exposure and environmental stressors, leading to excessive collagen and elastin degradation. This process accelerates wrinkle formation and reduces skin firmness [6]. Collagen contributes to the structure, elasticity, firmness, and flexibility of the skin. During aging, collagenase and elastase, which break down collagen and elastin, become more active. In turn, this results in wrinkles and a loss of skin elasticity. Therefore, agents that inhibit these enzymes can delay the formation of wrinkle and, thus, the aging process [7,8]. Hyaluronic acid is a substance mostly found in the skin and plays an important role in conserving moisture. Consequently, it plays an essential role in keeping hydration, plumpness, and elasticity of the skin, reducing the occurrence of wrinkles. Hyaluronic acid is a naturally occurring constituent in the body, mainly found in the skin and connective tissues. It plays a crucial role in retaining moisture, which makes it an essential component for maintaining skin hydration, plumpness, and elasticity. Hyaluronidase is an enzyme responsible for breaking down hyaluronic acid in tissues. Reduced hyaluronic acid synthesis, together with increased hyaluronidase activity, contributes to fine lines, wrinkles, and loss of skin firmness [7]. Tyrosinase is essential for melanin production. It initiates the transformation of L-tyrosine into L-DOPA, then its oxidation to L-dopaquinone which is converted to melanin by non-enzymatic processes. As tyrosinase plays a critical role in melanin synthesis, various inhibitors have been developed as treatments for hyperpigmentation disorders [9,10].

Therefore, an effective skin anti-aging strategy should focus on improving antioxidant activity along with inhibiting MMP, collagenase, elastase, hyaluronidase, and tyrosinase enzymes. Compared to synthetic alternatives, natural skin anti-aging treatments have several advantages. They are less likely to cause irritation or hypersensitivity reactions. Many natural products are safe and hardly to produce side effects. Indeed, this has led to an exponential increase in the research for the development of natural products that mitigate skin aging with the least adverse effects [11].

The selection of the plant was crucial because of the complex nature of the aging process, which involves various factors. The choice of *Astragalus sarcocolla* was guided by two main criteria supported by previous studies: its documented wound-healing potential and its antioxidant activity [12–14], both of

which are closely linked to mechanisms underlying skin aging. Accordingly, *A. sarcocolla* was considered a promising candidate for investigating skin anti-aging activity.

The genus *Astragalus* (family Fabaceae) is widely used in traditional medicine for the management of various health conditions [15]. *Astragalus sarcocolla* (commonly known as Anzaroot) is a shrub native to Iran (Persia), and its gum has been traditionally employed for the treatment of wounds, eye disorders, rheumatism, acne, inflammation, and bacterial infections [12,16]. Phytochemical investigations of the plant have reported the presence of bioactive constituents such as flavonoids, tannins, alkaloids, sterols, and terpenoids [16–18]. The *Astragalus* genus has been the subject of numerous chemical and biological studies, previous studies on *A. membranaceus* and *A. spinosus* that mainly focused on roots using conventional assays. In contrast, *A. sarcocolla* leaves remain largely unexplored, despite representing a sustainable and plant part with potentially distinct metabolic profiles [19].

Notably, no comprehensive or systematic study has yet evaluated the chemical composition and skin anti-aging potential of *A. sarcocolla* leaf extract (ASE). Therefore, the present work advances existing knowledge by (i) shifting the focus from the traditionally used gum to the leaf extract, (ii) providing a detailed metabolomic characterization of *A. sarcocolla* leaves, and (iii) integrating experimental bioassays with network pharmacology and molecular docking approaches. This integrated strategy enables a mechanistic understanding of how the identified metabolites interact with key skin anti-aging targets, including matrix metalloproteinase (MMP), collagenase, elastase, hyaluronidase, and tyrosinase. Collectively, this approach represents a novel contribution beyond previous studies on other *Astragalus* species and supports the potential of *A. sarcocolla* leaf extract as a new candidate for natural anti-aging skin applications.

2 Methods

2.1 Plant Material

Astragalus sarcocolla leaves were collected from Sakaka, Al-Jouf, Saudi Arabia, in February 2024 (geographical coordinates: 29.9697° N, 40.2065° E). Authentication of the plant sample was provided by Mr. Hamedan Al-Gereef, Camel Research Center, Al-Jouf, Saudi Arabia. For future reference, a voucher specimen (No. 75-CPJU) was kept at College of Pharmacy Herbarium, Jouf University.

2.2 Plant Extraction

The leaves were air-dried and ground into a powder. Two hundred grams of the powder were macerated with methanol (500 mL × 5) till exhaustion. The combined methanol extract was evaporated under vacuum (Buchi-210, Switzerland) to obtain a dried residue. All extractions were performed on a single batch, which was used for subsequent UPLC-MS analysis and biological assays. The extract (ASE) was stored in a tightly closed container at 4°C until use.

2.3 Chemicals

For enzymatic inhibition assays, porcine pancreatic elastase, collagenase (C8051), tricine buffer, succinyl-Ala-Ala-p-nitroanilide, the synthetic substrate N-[3-(2-furyl)acryloyl]-Leu-Gly-Pro-Ala (FALGPA, F5135), p-dimethylaminobenzaldehyde (PDMAB), mushroom tyrosinase, L-DOPA, phosphate buffer, acetate buffer, calcium chloride, sodium hydroxide, sodium borate, Tris-HCl buffer and calcium chloride buffer. For antioxidant assays, 2,2-diphenyl-1-picrylhydrazyl (DPPH), 2,4,6-tripyridyl-s-triazine (TPTZ), and ferric chloride were all obtained from Sigma Chemical Co. (St. Louis, MO, USA). Standards include epigallocatechin gallate (EGCG, Cat. E4143), butylated hydroxytoluene (BHT, Cat. W218405), tannic acid (Cat. 403040), kojic acid (Cat. K3125), and nordihydroguaiaretic acid (NDGA, Cat. 479975), obtained from Sigma. UPLC-MS

analysis was performed with HPLC-grade acetonitrile, methanol, and water provided by Thermo Fisher Scientific Inc. (Dublin, Ireland). The MMP-1 colorimetric kit (BML-AK404) was purchased from Enzo Life Sciences, and the MMP-9 colorimetric kit (ab139448) was obtained from Abcam. Other analytical-grade reagents were supplied by Sigma-Aldrich Chemical Co. (Ireland).

2.4 ASE Metabolite Profiling

Metabolite profiling of ASE was performed following a previously established method [20] using a Waters Acquity UPLC system (Waters, Manchester, UK) coupled with a high-resolution Orbitrap mass spectrometer (Exactive, Thermo Fisher Scientific, Bremen, Germany). Metabolite identification was achieved by comparing retention times, accurate masses, and fragmentation patterns (positive ionization mode) with published literature and database entries from the Dictionary of Natural Products (CRC Press). The mass accuracy was calculated as the difference between the observed and theoretical mass, expressed in ppm (0–10 ppm tolerance). When available, reference standards were used to confirm the identity of key compounds. Retention indices (RI) were recorded, and the identification confidence level for each compound was assigned according to MSI (Metabolomics Standards Initiative) guidelines: level 1 (confirmed with standard), level 2 (putatively annotated), or level 3 (putatively characterized class). Peak intensities in the UPLC–MS chromatogram represent relative abundances, not absolute concentrations.

2.5 Antioxidant Capacity

2.5.1 DPPH Assay

1,1-Diphenyl-2-picrylhydrazyl (DPPH) radical scavenging test was conducted according to a previously published method [21]. A 100 µL of various ASE concentrations (6.25–400 µg/mL) was combined with an equivalent amount of 0.06 mM DPPH prepared in absolute ethanol (99%). After a half-hour dark incubation period, the absorbance was measured at 517 nm with a microplate spectrometer (TECAN, Inc., NC, USA). Butylated hydroxytoluene (BHT) was used as the standard. DPPH radical scavenging capacity of ASE extract was estimated using the following Eq. (1)

$$\% \text{ Inhibition} = ((\text{Abs of control} - \text{Abs of ASE sample})/(\text{Abs of control})) \times 100 \quad (1)$$

2.5.2 FRAP Assay

ASE's ferric reducing antioxidant power (FRAP) was assessed according to the previously reported method [21], with minor modifications in sample concentration range and incubation conditions to optimize sensitivity for the plant extract. The FRAP solution was prepared by mixing 300 mM acetate buffer, 10 mM 2,4,6-tripyridyl-s-triazine (TPTZ), and 20 mM $FeCl_3 \cdot 6H_2O$ in a ratio of 10:1:1. The final mixture was incubated for 10 min at 37°C. Then, 3 mL of FRAP solution was mixed with 200 µL of ASE at different concentrations (50–250 µg/mL) and left at 37°C for 30 min. The absorbance of the formed colored complex was measured at 593 nm. Ascorbic acid was used as the reference standard, and results were expressed as µM $FeSO_4$ equivalent/g extract based on a ferrous sulfate calibration curve.

2.6 Enzyme Inhibitory Effect

2.6.1 Inhibition of MMP-1 and MMP-9

ASE inhibitory activity against matrix metalloproteinase-1 and 9 was assessed by MMP-1 and MMP-9 colorimetric kits. The assay was performed according to the manufacturer's protocol. Colorimetric measurement of enzyme activity was performed by monitoring the appearance of

oxidized N,N,N',N'-tetramethyl-p-phenylenediamine (TMPD) at 590 nm at various concentrations of ASE (25–500 µg/mL). N-Isobutyl-N-(4-methoxyphenylsulfonyl) glycyl hydroxamic acid (NNGH) was employed as reference control.

2.6.2 Collagenase Inhibition Activity

Collagenase inhibition testing was conducted using the method described earlier [22] with minor modifications. The assay mixture (100 µL) formed of *Clostridium histolyticum* collagenase (10 µL, 0.1 mg/mL), 30 µL of ASE (15.63–1000 µg/mL), and buffer tricine (60 µL of 50 mM tricine, pH 7.5, 10 mM calcium chloride, 400 mM sodium chloride) was prepared and kept at 37°C for 20 min. Then, 20 µL of N-[3-(2-furyl) acryloyl]-Leu-Gly-Pro-Ala substrate (1 mM FALGPA) was added to the mixture solution and the absorbance was determined after 15 min at 335 nm using a microplate reader (TECAN, Inc., NC, USA). EGCG was used as a standard, whereas the negative control mixture contained the enzyme (10 µL) with phosphate buffer (90 µL).

2.6.3 Elastase Inhibition Activity

The inhibition assay was conducted as described previously [22] with minor modifications. In brief, a 10 µL of porcine pancreatic elastase was blended with 25 µL of ASE (15.63–1000 µg/mL) and 100 mM Tris-HCl buffer (pH 8.0) and kept at 37°C for 5 min. The reaction was initiated by adding 20 µL of substrate solution (4.4 mM succinyl-Ala-Ala-Ala p-nitroanilide in Tris-HCl buffer). Absorbance was measured using a microplate reader (TECAN, Inc., NC, USA) at 410 nm. EGCG was used as a standard and distilled water as a negative control.

2.6.4 Hyaluronidase Inhibition Activity

Hyaluronidase inhibition activity was investigated using a previously published procedure [23] with modifications. A mixture of 50 µL of ASE (25–250 µg/mL) prepared in 10% DMSO was incubated with 10 µL hyaluronidase enzyme at 37°C for 10 min. Then, 20 µL of calcium chloride solution (12.5 mM) was added to the reaction and left for another 10 min at 37°C. Following, sodium hyaluronate (50 µL) was added to the reaction mixture and kept at 37°C for 40 min before mixing sodium hydroxide (0.9 M, 10 µL) and sodium borate (0.2 M, 20 µL). After incubation of the reaction mixture at 100°C for 3 min, *P*-dimethyl-amino-benzaldehyde (67 mM, 50 µL) was added and kept for another 10 min at 37°C. The absorbance was recorded at 585 nm. Tannic acid served as the reference standard and distilled water as a negative control.

2.6.5 Tyrosinase Inhibition Activity

Inhibition of tyrosinase was assayed using an established method [24]. Mushroom tyrosinase (10 µL, 50 units/mL) aqueous solution was mixed with phosphate buffer (pH 6.8, 80 µL) and ASE (20 µL, 25–250 µg/mL) and kept at 37°C for 5 min. Then, L-DOPA (90 µL, 2 mg/mL) was added and the reaction mixture was incubated again for 20 min at the same temperature. The concentration of produced dopachrome was measured spectrophotometrically at 475 nm. Phosphate buffer was served as a blank, and kojic acid was a standard.

The percentage inhibitory effect on collagenase, elastase, hyaluronidase, and tyrosinase was determined using Eq. (1).

2.7 Statistical Analysis

All assays were performed as three independent experiments. Results are expressed as mean ± standard deviation (SD). Data analysis was conducted using Microsoft Excel 2010 and GraphPad Prism software version 8 (San Diego, CA). Dose–response curves were generated and analyzed using non-linear regression to accurately determine the 50% inhibitory concentration (IC_{50}).

2.8 Network Pharmacology

2.8.1 Screening of Identified Metabolites and Their Target Genes

Metabolites identified by UPLC-MS were scrutinized for their drug likeness (DL) and bioavailability (F) properties. To satisfy ADME criteria, metabolites were retained only if their DL was ≥0.18 and F was ≥30%. SwissADME and ADMETlab were used to calculate the F30% and DL values for each active metabolite [25]. The potential molecular targets of ASE metabolites were predicted by Swiss Target Prediction [26] and STITCH platform [27]. The metabolites were screened in the STITCH platform with a focus on 'Homo sapiens' to identify targets. Only those possessing an average score of ≥0.7 were chosen for subsequent analyses. Furthermore, the SMILES value of each metabolite was imported to Swiss Target Prediction online platform. Reverse pharmacophore matching was used to identify drug target names. Targets with probability ≥ 0.7 were chosen.

2.8.2 Screening of Disease Related and Overlapping Target Genes

The first step in elucidating the molecular mechanisms underlying herbal medicines' effectiveness in treating various diseases is to identify genes linked to a particular disease. Trying to extract genes associated with skin aging, GeneCard [28] and Online Mendelian Inheritance in Man (OMIM) databases were searched using the keyword 'skin aging'. Moreover, these platforms supply detailed genomic information and functional annotations of the known human genes. Streamlining the process involved removing redundant genes from the final set. Subsequently, UniProtKB [29] was searched to find the recognized names of the target genes, designating the species 'Homo sapiens'. The anticipated target genes of selected ASE metabolites were then compared with skin aging-related targets, and a Venn diagram was crafted to pinpoint common targets for subsequent analysis.

2.8.3 Protein-Protein Interaction Network Construction

Protein-protein interactions are of great importance owing to their remarkable versatility, adaptability, and specificity. STRING (Retrieval of Interacting Genes/Proteins tool) was used to identify functional interactions between relevant targets characterized by an average score exceeding 0.7. The PPI network was then analyzed by the CytoHubba plugin integrated into Cytoscape. This strategy enabled the identification of key regulatory genes in the PPI network and key targets [30].

2.8.4 Functional Enrichment and Pathway Analysis

The key targets were evaluated as part of function prediction at three domains: biological process (BP), molecular function (MF), and cellular component (CC). A significance threshold of adjusted p-value ≤ 0.05 was applied, and the top ten GO enrichments and top ten KEGG pathways with the highest scores were highlighted for a more thorough investigation [30].

2.9 Molecular Docking

Key targets were established via molecular docking studies. RCSB Protein Data Bank (global database of protein and nucleic acid 3D structures) was used to retrieve X-ray crystal structures of targets. Then, structures were refined using Chimera [31]. Active site residues were identified through CASTp software, while PyRx software supported target docking between key targets and active metabolites [32]. The finding of the optimum docking pose, marked by the lowest root mean square deviation (RMSD) and binding energy, was essential for subsequent investigations. Docking scores between key targets and metabolites were used as significant assessment indicators to identify relevant constituents and their respective targets. When assessing the docked complexes, models exhibiting the highest value of binding energy and best stability were assumed to be reliable. Also, Chimera X and Discovery Studio were implemented for visualization of interactions between active metabolites and anticipated targets [33].

3 Results and Discussion

3.1 Metabolite Profiling of ASE

The UPLC-MS analysis (Fig. S1) led to the detection of twenty-seven metabolites in ASE. The extract was analyzed in positive ESI mode to uncover the phytochemical profile (Table 1). Flavonoids were the predominant group (15), followed by phenolic acid and phenolic acid derivatives (8), and coumarins (4). Flavonoids of different subclasses were detected in the extract. Five metabolites (acacetin, luteolin, apigenin, 7,3′,4′,5′-tetrahydroxyflavone, and luteolin-5-O-β-glucoside) belong to the flavone subclass (peaks 3, 8, 10, 15, and 18) [34–36]. Another five metabolites (kaempferol, morin, myricetin, quercetin, and hyperin) were identified as flavonols (peaks 6, 11, 19, 22, and 24) [37–39]. A single flavanonol, aromadendrin (peak 5), was also annotated [40]. Four metabolites, namely isoliquiritigenin, licochalcone A, licochalcone B, and naringin were identified as chalcones or flavanone derivatives (peaks 7, 20, 21, and 26) [41–44].

In addition, several phenolic acids (peaks 1, 2, 9, 12, 13, 14, 23, and 27) were annotated: gallic, caffeic, sinapic, ellagic, syringic, cinnamic, rosmarinic acids and ethyl ferulate which mainly belong to the hydroxycinnamic and hydroxybenzoic acid groups [45–47]. Four coumarin derivatives (peaks 4, 16, 17, and 25) were also detected, including xanthoxylin, isofraxidin, scoparone, and scopoletin [48–51].

Flavonoids such as luteolin, kaempferol, and apigenin are among the identified compounds and have been extensively reported for their anti-inflammatory, antioxidant, and anti-collagenase properties [52,53]. This is the first study to thoroughly explore the metabolite profile of ASE. The chemical composition of ASE is not well documented in the literature; however, the other parts of the plant contain flavonoids, tannins, alkaloids, sterols, and terpenoids [16–18].

Table 1: Metabolites identified in *Astragalus sarcocolla* leaves extract analyzed by UPLC-MS in positive ion mode.

ID	*Rt (min.)	(M+H)	Molecular Formula	Error (ppm)	Ms/Ms	Metabolite	Chemical Class	RI	Confidence Level
1	1.56	170.0357	$C_7H_6O_5$	−0.52	153, 127	Gallic acid	Phenolic acid	1200	Level 2
2	1.83	180.0677	$C_9H_8O_4$	3.33	135	Caffeic acid	Phenolic acid	1230	Level 2
3	2.11	284.0633	$C_{16}H_{12}O_5$	−4.59	270, 243	Acacetin	Flavone	1300	Level 2
4	2.22	196.0685	$C_{10}H_{12}O_4$	−4.54	167, 138	Xanthoxylin	Coumarin	1250	Level 2
5	2.35	288.0670	$C_{15}H_{12}O_6$	4.18	153, 243	Aromadendrin	Flavanonol	1310	Level 2
6	2.53	286.0532	$C_{15}H_{10}O_6$	5.9	165, 120	Kaempferol	Flavonol	1320	Level 2
7	2.55	256.0809	$C_{15}H_{12}O_4$	2.02	239, 147, 137, 119,111	Isoliquiritigenin	Chalcone	1280	Level 2
8	2.66	286.0694	$C_{15}H_{10}O_6$	1.05	148	7,3′,4′,5′-Tetrahydroxyflavone	Flavone	1330	Level 2
9	2.78	222.0874	$C_{12}H_{14}O_4$	−1.24	195, 177	Ethyl ferulate	Phenolic acid	1270	Level 2
10	2.84	286.0438	$C_{15}H_{10}O_6$	−3.32	257	Luteolin	Flavone	1340	Level 2
11	2.85	302.0323	$C_{15}H_{10}O_7$	−0.04	271, 229, 151	Morin	Flavonol	1350	Level 2
12	2.97	224.0919	$C_{11}H_{12}O_5$	2.81	207, 175	Sinapic acid	Phenolic acid	1260	Level 2
13	3.34	302.0202	$C_{14}H_6O_8$	−0.78	285, 257, 201	Ellagic acid	Phenolic acid	1290	Level 2
14	3.43	198.0746	$C_9H_{10}O_5$	1.17	155, 123	Syringic acid	Phenolic acid	1245	Level 2
15	3.81	270.0517	$C_{15}H_{10}O_5$	−0.57	227, 151, 117	Apigenin	Flavone	1360	Level 2
16	3.90	222.0766	$C_{11}H_{10}O_5$	3.04	207, 179	Isofraxidin	Coumarin	1285	Level 2
17	4.03	206.0461	$C_{11}H_{10}O_4$	3	152	Scoparone	Coumarin	1275	Level 2
18	4.25	448.0643	$C_{21}H_{20}O_{11}$	2.08	286, 244	Luteolin-5-O-β-glucoside	Flavone	1380	Level 2
19	4.53	318.0402	$C_{15}H_{10}O_8$	3.14	192, 133	Myricetin	Flavonol	1390	Level 2
20	4.70	286.0918	$C_{16}H_{14}O_5$	1.05	249, 183, 117	Licochalcone B	Chalcone	1370	Level 2
21	4.81	338.1344	$C_{21}H_{22}O_4$	−1.54	297, 121	Licochalcone A	chalcone	1375	Level 2
22	5.31	302.0373	$C_{15}H_{10}O_7$	−4.76	178, 151	Quercetin	Flavonol	1400	Level 2
23	5.83	148.0474	$C_9H_8O_2$	2.45	120, 102	Cinnamic acid	Phenolic acid	1255	Level 2
24	6.42	465.0654	$C_{21}H_{20}O_{12}$	4.96	303, 285, 163	Hyperin	Flavonol	1410	Level 2
25	6.99	192.0418	$C_{10}H_8O_4$	0.11	166, 103	Scopoletin	Coumarin	1295	Level 2
26	9.06	581.2744	$C_{27}H_{32}O_{14}$	−5.95	273,191, 147, 103	Naringin	Flavanone	1420	Level 2
27	9.23	360.0789	C18H16O8	−4.92	197, 162, 135	Rosmarinic acid	Phenolic acid	1265	Level 2

*Rt: retention time.

3.2 Antioxidant Capacity

One of the main origins of skin aging is UV radiation exposure, which induces the production of reactive oxygen species (ROS). This leads to oxidative stress, degradation of collagen and elastin in the extracellular matrix (ECM), and inflammation, which speed up the aging process. As a result, antioxidant supplements are used to shield the skin from environmental toxins, helping to reduce oxidative stress and prevent premature aging [54]. The antioxidant activity of ASE was evaluated using two *in vitro* assays. In the DPPH radical scavenging assay, ASE showed a significant antioxidant capacity (Table 2). ASE extract effectively scavenged DPPH radical, with an IC_{50} of 26.050 ± 0.656 µg/mL, compared to BHT's IC_{50} of 19.945 ± 0.120 µg/mL. In the FRAP assay, ASE also exhibited promising reducing power, with a value of 2433.00 ± 3.00 µM $FeSO_4$/g extract, while ascorbic acid (positive control) had a value of 4801.3 ± 1.527 µM $FeSO_4$/g extract (Table 2).

Table 2: DPPH radical scavenging and FRAP antioxidant capacities of *Astragalus sarcocolla* leaves extract.

	DPPH[a] (IC_{50}, µg/mL)	**FRAP[b] (µM $FeSO_4$/g extract)**
Astragalus sarcocolla leaf extract (ASE)	26.050 ± 0.656	2433.00 ± 3.00
BHT (butylated hydroxytoluene)	19.945 ± 0.120	-
Ascorbic acid	-	4801.3 ± 1.416

a: 2,2-Diphenyl-1-picrylhydrazyl; b: Ferric reducing antioxidant power; All data are presented as mean ± SD.

The antioxidant activities of ASE observed in DPPH and FRAP assays are consistent with recent studies on *Astragalus* species. *Astragalus membranaceus* extracts have been shown to exhibit significant free-radical scavenging and reducing power in antioxidant assays, attributed to their phenolic and flavonoid constituents [55]. Phenolic compounds are well known for their ability to prevent or slow skin aging by combating oxidative stress [56]. The UPLC-MS analysis confirmed the presence of such antioxidant-rich metabolites in ASE, supporting its observed activity. These findings align with previous reports showing that phenolic-rich plant extracts can effectively protect against skin aging [57,58].

3.3 Enzyme Inhibition Activity

3.3.1 MMP-1 and MMP-9 Inhibition Activity

Metalloproteinases (MMPs) are enzymes that break down the extracellular matrix (ECM) and play a role in dermal remodelling and turnover. Although there are many types of MMP, only some are linked to skin wrinkles. These include collagenases (MMP-1), which degrade collagen, and gelatinases (MMP-9), which break down denatured collagen [10]. Table 3 represents ASE's inhibitory effects on these MMPs. ASE demonstrated significant inhibition of MMP-1 and MMP-9, with notable effects at higher concentrations. MMP-1 inhibition increased from 56.92% at 25 µg/mL to 76.92% at 500 µg/mL, while MMP-9 inhibition rose from 46.58% at 25 µg/mL to 78.08% at 500 µg/mL. These results were compared with NNGH (N-Isobutyl-N-(4-methoxyphenylsulfonyl)-glycyl-hydroxamic acid), which showed inhibition rates of 92.31% and 95.89%, respectively, at a concentration of 1.3 µM.

Table 3: MMP-1 and MMP-9 inhibition (%) of *Astragalus sarcocolla* extract (ASE), NNGH was 92.31% and 95.89%, respectively at 1.3 µM concentration.

	MMP-1 Inhibition %				**MMP-9 Inhibition %**			
	25	**50**	**250**	**500**	**25**	**50**	**250**	**500**
ASE	56.92	63.08	73.85	76.92	46.58	57.53	69.86	78.08

The ECM, which is primarily made up of elastic fibers and collagen, provides the structural framework for the skin. Prolonged UV exposure induces the development of MMPs in epidermal keratinocytes, which accelerates skin sagging and wrinkle formation by breaking down extracellular matrix proteins and collagen. MMP-1 specifically breaks down type I and type III collagen, which are crucial for maintaining skin strength and elasticity. Increased MMP-1 activity contributes to the loss of skin firmness and the formation of wrinkles due to accelerated degradation of these collagen types. This is often exacerbated by environmental factors such as UV radiation, which can upregulate MMP-1 production. MMP-9 degrades type IV and type V collagen as well as some non-collagenous components of the ECM. It is involved in various physiological processes, including wound healing and tissue remodeling. MMP-9 activity can be triggered by inflammatory responses, UV exposure, and other stressors. Chronic activation of MMP-9 can lead to the breakdown of the ECM components, contributing to skin thinning, increased wrinkle formation, and loss of elasticity [2,10]. The results confirmed the potential for ASE as an effective agent for inhibiting MMP, which could contribute to the prevention of wrinkle formation.

3.3.2 Collagenase, Elastase, Hyaluronidase, and Tyrosinase Inhibition

Moreover, ECM breakdown is correlated with the increased activity of collagenase, elastase, and hyaluronidase enzymes. Even though tyrosinase does not directly participate in skin structural aging, it is associated with pigmentation disorders like age spots or hyperpigmentation during aging [59]. UV radiation can boost the activity of these enzymes thereby contributing to the degradation of the ECM and appearance of signs of premature aging [21,54].

Therefore, inhibiting these enzymes offers a promising approach to combat aging, delay visible signs like wrinkles and hyperpigmentation, and holds potential in dermatological and cosmetic treatments [5]. Hence, ASE was tested for its ability to inhibit these four key skin-remodeling enzymes. As shown in Fig. 1, ASE had the strongest effect on collagenase, almost matching the standard inhibitor EGCG (IC_{50} 35.038 ± 0.386 μg/mL vs. 32.069 ± 2.731 μg/mL). It also significantly inhibited elastase (IC_{50} 40.748 ± 0.758 μg/mL vs. 32.948 ± 0.178 μg/mL for EGCG), but had weaker effects on hyaluronidase IC_{50} 61.389 ± 1.635 μg/mL vs. 30.213 ± 0.430 μg/mL for tannic acid) and tyrosinase (IC_{50} 30.980 ± 0.918 μg/mL vs. 16.395 ± 0.283 μg/mL for kojic acid). Enzyme inhibitory data for other *Astragalus* species support the capacity of this genus to modulate enzymes related to aging and oxidative stress, aligning with our findings on collagenase and elastase inhibition by ASE [60].

The observed antioxidant and enzyme inhibition activities of ASE can be mechanistically attributed to its major metabolites. Kaempferol and luteolin are well-known antioxidants that scavenge free radicals and enhance cellular antioxidant defenses [61], likely contributing to the strong DPPH and FRAP responses. Rosmarinic acid has been reported to inhibit elastase activity, supporting the observed enzyme inhibition results [62]. Additionally, apigenin and acacetin have documented anti-inflammatory and enzyme-modulatory effects consistent with inhibition of MMP-related pathways [63,64]. These findings suggest that the bioactivities of ASE are the result of multiple metabolites acting synergistically on key targets associated with skin aging.

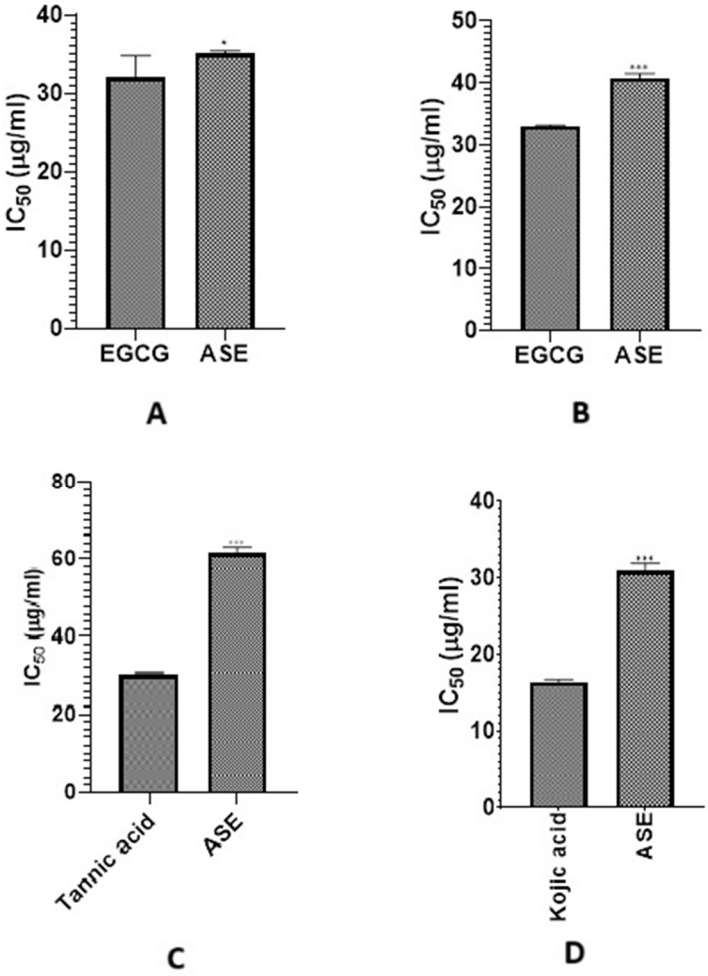

Figure 1: IC_{50} of ASE against (**A**) collagenase, (**B**) elastase, (**C**) hyaluronidase, (**D**) tyrosinase compared to their corresponding positive controls. Values of p lower than 0.05 were considered statistically significant. The vertical bars represent mean ± standard deviation (SD), while * and *** indicate statistical significance, corresponding to $p < 0.05$ and $p < 0.001$, respectively, compared with the control/reference group.

3.4 Network Pharmacology

Network pharmacology is an advanced technique that uses systems biology and bioinformatics to investigate the complex relationships between bioactive chemicals, target genes, and biological pathways. In contrast to classical pharmacology, which focusses on a single site, network pharmacology emphasizes drugs' multi-target effects, offering a full view of their therapeutic potential. This method is particularly beneficial for studying natural products such as plant extracts since it enables the discovery of key chemicals, target genes, and roles within interlinked signalling networks linked to a variety of disorders, including skin ageing [65,66].

3.4.1 Screening of Identified Compounds and Target Gene Prediction

Twenty-seven compounds identified by UPLC-MS were first screened on the basis of two criteria of DL and OB. Candidate compounds were screened based on drug-likeness (DL) ≥ 0.18 and oral bioavailability (OB) ≥ 30%, which are widely accepted thresholds in network pharmacology studies [67]. These criteria

ensure the selected compounds have a higher likelihood of being pharmacologically active and bioavailable *in vivo*, thus making them relevant for investigating potential skin anti-aging effects.

Out of 27 compounds, 24 compounds met the aforementioned filtering criteria and only three compounds namely licochalcone A, syringic acid and xanthoxylin were removed from the list. OB and DL values of these compounds are mentioned in Table S1. Afterwards, target genes for these 24 compounds were identified and three compounds namely aromadendrin, luteolin-5-O-β-glucoside and sinapic acid did not displayed any target gene so were also excluded. At the end there were total 21 compounds which targeted 359 genes. The details about target genes of each compound are presented in Table S2.

Afterward 956 skin anti-aging target genes (Table S3) were identified from geneCards and intersecting genes between identified compounds and anti-aging gene were estimated using Venn diagram as shown in Fig. 2. A total of 66 intersecting genes were screened. The names of intersecting genes are provided in Table S4.

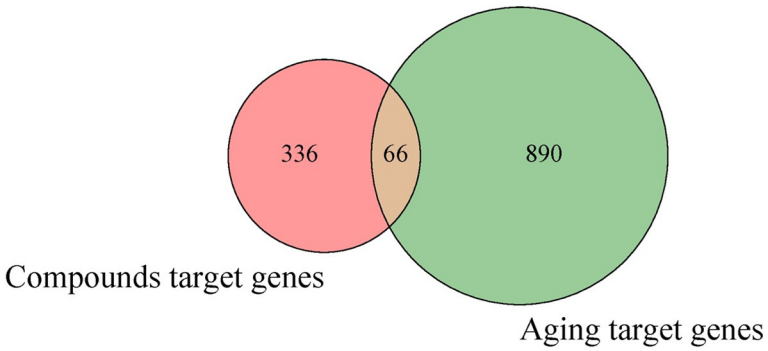

Figure 2: Venn diagram representing overlapping genes between selected identified compounds in ASE and skin aging related genes.

3.4.2 Compound-Compound Target Genes Network Analysis

A network was constructed among selected compounds and their target genes especially those target genes which are present in list of overlapping genes. This was done to predict the most potent compounds which can target aging related genes. Degree value was assigned to each compound in order to predict the most contributing compounds that might be responsible for anti-aging effect of ASE. Greater the degree value greater will be the possibility of compound to be considered as key compound responsible for anti-aging attribute. Top five compounds (Fig. 3) screened by Cytohubba plugin were cinnamic acid (35), acacetin (25), luteolin (25), kaempferol (24) and apigenin (24). These compounds were then selected for further analysis in molecular docking.

3.4.3 PPI Network Analysis

PPI Network analysis revealed that among 66 intersecting genes, top ten genes include TNF (50), MMP-9 (43), ESR1 (42), PTGS-2 (39), EGFR (39), CCND1 (36), MMP-2 (34), SRC (34), ERBB2 (33) and TLR4 (32). The greater degree value of these genes denotes that they showed strong inter relationship with other genes thereby are considered to be the hub genes that might be responsible for skin aging effects. Among all these genes, MMP-9, ESR1, PTGS-2 and EGFR were targeted by majority of selected compounds thereby these genes were selected for molecular docking analysis.

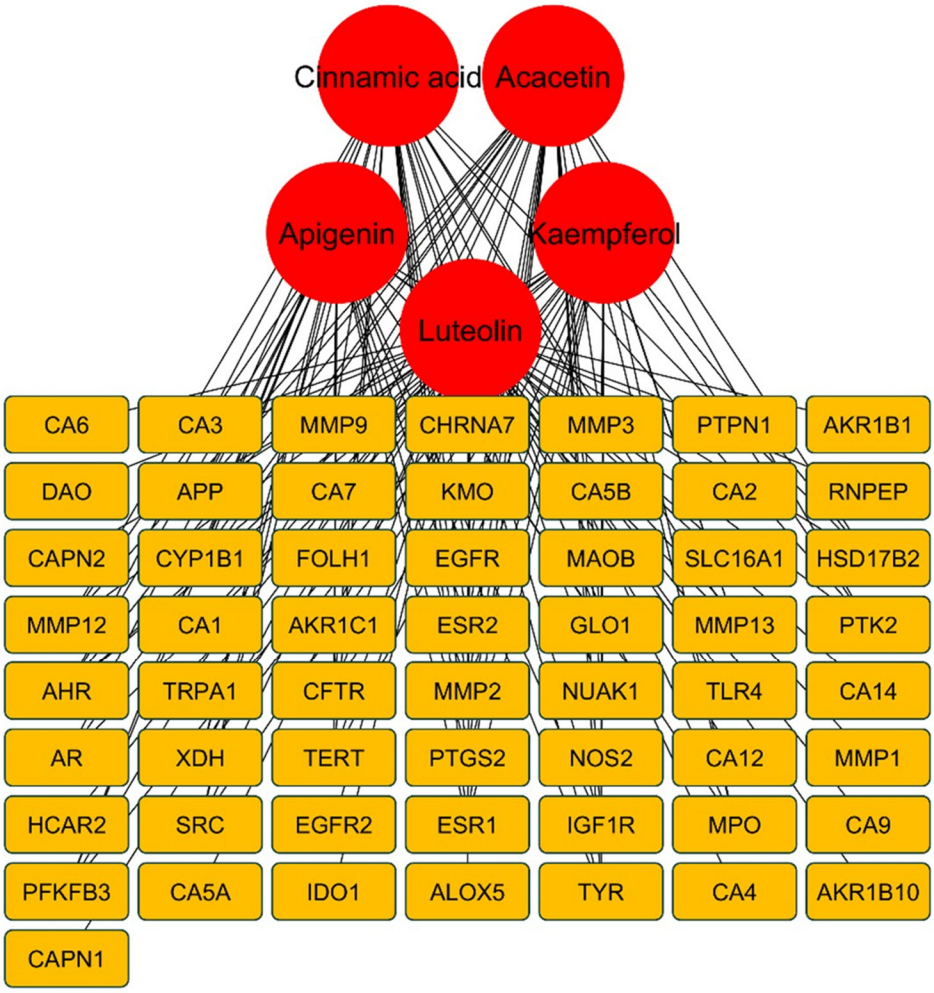

Figure 3: Genes targeted by the screened top five metabolites of ASE.

3.4.4 GO and KEGG Pathway Analysis

The functional annotation and enrichment analysis provided insights into the potential biological functions of Anzaroot targets. GO functional analysis (Fig. 4A) indicated that these targets were involved in processes such as collagen metabolism, extracellular matrix disassembly, and response to oxidative stress. KEGG pathway analysis (Fig. 4B) aimed to identify significant signaling pathways connected to ASE's skin anti-aging properties. Notably, numerous genes were involved in pathways including proteoglycans in cancer (16), endocrine resistance (15), lipid and atherosclerosis (14), relaxin signaling pathway (12), and FoxO signaling pathway (12). Finally, KEGG pathway analysis revealed significant enrichment of genes such as MMP-9, PTGS-2, and EGFR.

Network pharmacology revealed that 21 of out of 27 compounds identified in ASE targeted 66 genes associated with skin aging. Among these, MMP-9, PTGS-2, and EGFR emerged as hub genes with the highest degree values, indicating their central role in skin anti-aging mechanisms. MMP-9 plays a critical role in extracellular matrix degradation by cleaving collagen and elastin fibers, contributing to wrinkle formation and loss of skin firmness during intrinsic and photo-induced aging [68]. PTGS-2 (COX-2) is a central mediator of inflammation and oxidative stress in aged and photo-damaged skin, and its overexpression is associated with accelerated skin aging and impaired tissue repair [69]. EGFR is essential for keratinocyte

proliferation, epidermal regeneration, and wound healing, and dysregulation of EGFR signaling has been linked to impaired skin renewal and aging phenotypes [70].

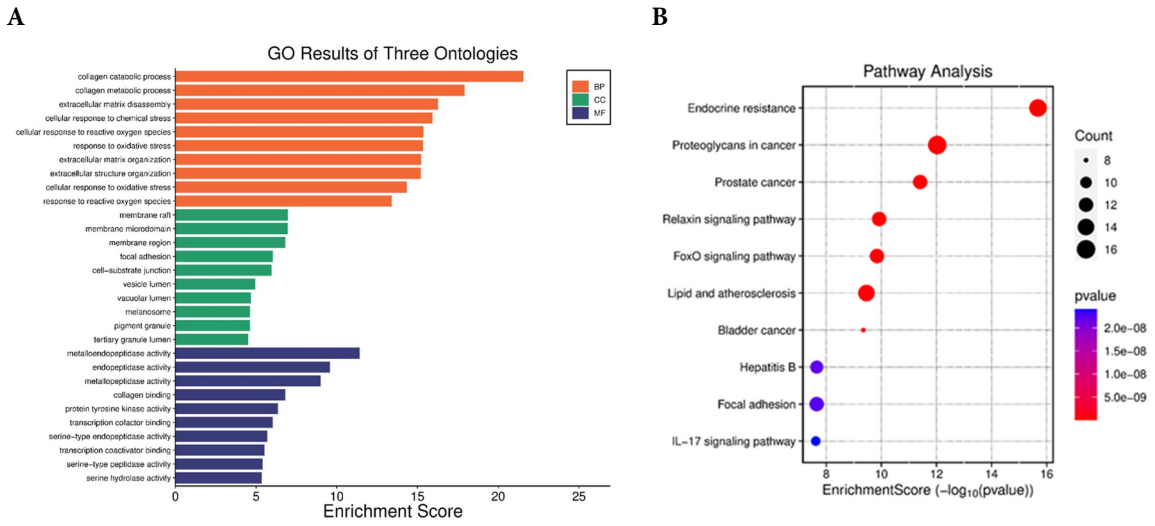

Figure 4: (**A**) GO enrichment analysis and (**B**) KEGG pathway enrichment analysis of overlapping genes.

KEGG pathway enrichment highlighted FoxO and Nrf2 signaling pathways. These signaling pathways play important roles in controlling antioxidant defenses and cellular stress responses. FoxO transcription factors regulate the expression of genes encoding antioxidant enzymes, contributing to cellular protection against oxidative stress and maintenance of redox homeostasis [71]. Likewise, Nrf2 acts as a regulator of antioxidant and cytoprotective genes, helping to mitigate oxidative damage and promote cellular protection [72].

3.5 Molecular Docking

In order to find possible mechanisms of action for selected target genes (MMP-9 1GKC, ESR1 1A52, PTGS-2 5F19 and EGFR 4ZAU) and metabolites (cinnamic acid, acacetin, luteolin, kaempferol and apigenin), a molecular docking analysis was performed (Figs. S2–S4). None of the selected five compounds displayed significant interactions with ESR1. Docking scores and binding energy were the primary parameters for evaluating compounds, as presented in Table 4.

Clusters with the highest absolute binding energy and the most stable conformations were chosen. The proteins MMP-9, PTGS-2, and EGFR demonstrated the greatest binding energy and RMSD with acacetin and apigenin. Therefore, the results suggest that ASE active metabolites stably bind to the proteins of all three targets, acting as inhibitors of skin aging. Furthermore, it is important to explore how the active metabolites interact with the three targets to understand their mechanism of action in more detail. All selected metabolites showed hydrogen bonds, Pi-PI stacking, and van der Waals interactions with the receptor proteins, indicated by dotted lines (Figs. S2–S4). Analysis of the binding interactions revealed that acacetin and apigenin exhibited stronger affinities for MMP-9, PTGS-2, and EGFR than the other constituents as shown in Figs. S2–S4.

Table 4: Binding mode analysis of top five metabolites into the binding pocket of MMP-9, PTGS-2 and EGFR.

Target Genes	Compounds	RMSD	Binding Affinity (kcal/mol)	Interacting Residues of Active Site
MMP-9	Acacetin	2.34	−7.135	HIS401, ARG424, ALA417, TYR423, LEU418, VAL398
	Cinnamic acid	2.46	−5.3486	HIS401, TYR423,
	Luteolin	1.63	−6.9417	PRO421, ARG424, LEU418, HIS401,
	Kaempferol	0.93	−6.4023	HIS401, ARG424, LEU397, VAL398,
	Apigenin	1.78	−6.9954	HIS411, PRO421, GLU402, ALA417, LEU418, HIS401, ARG424
PTGS-2	Acacetin	0.74	−4.5539	ASP133, PHE220, TYR147, TYR143
	Cinnamic acid	1.20	−3.7083	TRP139, ASN144
	Luteolin	1.87	−4.5086	SER143, GLU140
	Kaempferol	2.85	−4.4372	SER146, ASN144, GLU140
	Apigenin	1.20	−4.4729	GLU140
EGFR	Acacetin	0.97	−5.956	LEU718, VAL726, LYS745, LEU788, ALA743, LEU792, MET793, LEU844, THR854, GLU762
	Cinnamic acid	0.87	−4.589	VAL726, LYS745, ALA743, ASP855
	Luteolin	1.60	−5.586	LEU844, GLN791, CYS755, GLU762, LYS745
	Kaempferol	2.14	−5.668	LYS745, MET793, LEU844, ALA743, LEU718
	Apigenin	1.07	−5.549	LEU718, VAL726, ALA743, GLN791, CYS775, LEU844

The predicted strong binding affinities of acacetin and apigenin toward MMP-9, PTGS-2, and EGFR in this study are consistent with previous molecular docking analyses of these flavonoids. For example, apigenin has been shown to bind with high affinity to MMP-9 and PTGS-2 in a network pharmacology model, suggesting effective interaction with inflammatory and matrix-degrading enzymes [73]. Similarly, acacetin has demonstrated favorable docking interactions with PTGS-2 and EGFR in earlier computational studies, supporting its potential to modulate inflammation and proliferative signaling pathways [74].

The strong binding affinities predicted for acacetin and apigenin with MMP-9 suggest potential inhibition of this protease, which could mitigate excessive extracellular matrix (ECM) degradation. Similarly, high affinities toward PTGS-2 (COX-2) indicate possible attenuation of pro-inflammatory signaling, aligning with a reduction in oxidative stress and chronic inflammation, key drivers of aging. Finally, interactions with EGFR may support epidermal repair and renewal mechanisms.

The integration of *in vitro* enzyme inhibition assays with molecular docking analysis provides complementary evidence supporting the skin anti-aging potential of ASE. Among the identified metabolites, acacetin and apigenin consistently exhibited the highest binding affinities toward MMP-9, PTGS-2, and EGFR. These targets are directly associated with extracellular matrix degradation, inflammation, and skin aging processes. Importantly, the strong *in silico* binding affinities of acacetin and apigenin correlate with the pronounced inhibitory effects observed experimentally against skin aging-related enzymes, including MMPs, collagenase, elastase, and tyrosinase. This concordance between experimental and computational results supports the hypothesis that ASE exerts its anti-aging activity through a multi-target synergistic mechanism, rather than a single-enzyme mode of action. The pharmacological significance of these metabolites should be further investigated in preclinical and clinical studies to support their integration into future therapeutic or cosmetic applications.

The current study is limited to *in vitro* and computational analyses, which may not fully reflect biological effects in living systems. Future cell-based studies (e.g., fibroblasts, keratinocytes) and *in vivo* experiments are needed to validate these findings. Additionally, the potential synergistic interactions among major flavonoids such as acacetin, luteolin, and apigenin could be explored to better understand their combined contribution to skin anti-aging effects.

4 Conclusions

This study investigated the phytochemical composition and skin anti-aging potential of *Astragalus sarcocolla* leaf extract (ASE). UPLC-MS analysis identified numerous phenolic compounds, including flavonoids and phenolic acids. Moreover, ASE demonstrated robust antioxidant properties and inhibited skin aging-related enzymes (MMP-1, MMP-9, collagenase, elastase, hyaluronidase, and tyrosinase). Network pharmacology analysis uncovered the interaction of ASE constituents with key target genes including MMP-9, ESR1, PTGS-2, and EGFR involved in aging. Docking studies showed that acacetin and apigenin displayed the highest affinities for MMP-9, PTGS-2, and EGFR, supporting their multi-target inhibitory activity. Future investigations should aim to clarify the underlying mechanisms of action and assess the *in vivo* efficacy of these compounds. In conclusion, these findings highlight ASE as a promising natural source of bioactive phenolics that possess skin anti-aging properties. Further investigations may help incorporate ASE into cosmetics for fighting and delaying skin aging. Our results pave the way for the inclusion of ASE in anti-aging products. To validate the *in vitro* results, further *in vivo* biological studies using topical formulations containing ASE are planned.

Acknowledgement: Not applicable.

Funding Statement: This work was funded by the Deanship of Graduate Studies and Scientific Research at Jouf University under grant No. (DGSSR-2023-01-02126).

Author Contributions: The authors confirm contribution to the paper as follows: Conceptualization, Shaimaa R. Ahmed; Methodology, Shaimaa R. Ahmed and Omnia M. Hendawy; Investigation, Sumera Qasim, Hanan Khojah, Ambreen Malik Uttra; Data curation and analysis, Shaimaa R. Ahmed and Hanan Khojah; Visualization, Sumera Qasim and Ambreen Malik Uttra; Writing-original draft preparation, Shaimaa R. Ahmed; Writing-review and editing, Shaimaa R. Ahmed, Omnia M. Hendawy, Sumera Qasim, Hanan Khojah, Ambreen Malik Uttra; Supervision, Shaimaa R. Ahmed; Project administration, Shaimaa R. Ahmed; Funding acquisition, Shaimaa R. Ahmed. All authors reviewed and approved the final version of the manuscript.

Availability of Data and Materials: Data available on request from the authors.

Ethics Approval: Not applicable.

Conflicts of Interest: The authors declare no conflicts of interest.

Supplementary Materials: The supplementary material is available online at https://www.techscience.com/doi/10.32604/phyton.2026.075718/s1. Figure S1: Total ion chromatogram of *Astragalus sarcocolla* leaf extract recorded in positive ionization mode. Figure S2: Molecular docking of compounds with MMP-9. Figure S3: Molecular docking of compounds with PTGS-2. Figure S4: Molecular docking of compounds with EGFR. Table S1: OB and DL values of identified compounds. Table S2: Target genes of each compound. Table S3: Skin anti-aging target genes. Table S4: Intersecting genes between identified compounds and skin anti-aging gene.

Abbreviations

ADME	Absorption, Distribution, Metabolism, and Excretion
BHT	Butylated hydroxytoluene
DL	Drug-likness
DPPH	2,2-Diphenyl-1-picrylhydrazyl
ECM	Extracellular matrix
EGCG	Epigallocatechin gallate
EGFR	Epidermal Growth Factor Receptor

ESR1	Estrogen Recetor 1
FRAP	Ferric Reducing Antioxidant Power
MMPs	Matrix Metalloproteinases
NNGH	N-Isobutyl-N-(4-methoxyphenylsulfonyl) glycyl hydroxamic acid
OB	Oral bioavailability
ROS	Reactive oxygen species
UPLC-MS	Ultraperformance Liquid Chromatography-Mass Spectrometry

References

1. Chaiyana W, Chansakaow S, Intasai N, Kiattisin K, Lee K-H, Lin W-C, et al. Chemical constituents, antioxidant, anti-MMPs, and anti-hyaluronidase activities of *Thunbergia laurifolia* Lindl. leaf extracts for skin aging and skin damage prevention. Molecules. 2020;25(8):1923. [CrossRef].
2. Uzun M, Demirezer L. Anti-aging power of *Rumex crispus* L.: matrix metalloproteinases inhibitor, sun protective and antioxidant. S Afr J Bot. 2019;124:364–71. [CrossRef].
3. Hussein RS, Bin Dayel S, Abahussein O, El-Sherbiny AA. Influences on skin and intrinsic aging: biological, environmental, and therapeutic insights. J Cosmet Dermatol. 2025;24(2):e16688. [CrossRef].
4. Maestri E. The 3Rs principle in animal experimentation: a legal review of the state of the art in Europe and the case in Italy. BioTech. 2021;10(2):9. [CrossRef].
5. Cruz AM, Gonçalves MC, Marques MS, Veiga F, Paiva-Santos AC, Pires PC. *In vitro* models for anti-aging efficacy assessment: a critical update in dermocosmetic research. Cosmetics. 2023;10(2):66. [CrossRef].
6. Chen J, Qin S, Liu S, Zhong K, Jing Y, Wu X, et al. Targeting matrix metalloproteases in diabetic wound healing. Front Immunol. 2023;14:1089001. [CrossRef].
7. Altyar AE, Ashour ML, Youssef FS. *Premna odorata*: Seasonal metabolic variation in the essential oil composition of its leaf and verification of its anti-ageing potential via *in vitro* assays and molecular modelling. Biomolecules. 2020;10(6):879. [CrossRef].
8. Madan K, Nanda S. *In-vitro* evaluation of antioxidant, anti-elastase, anti-collagenase, anti-hyaluronidase activities of safranal and determination of its sun protection factor in skin photoaging. Bioorg Chem. 2018;77:159–67. [CrossRef].
9. Lu YF, Tonissen K, Di Trapani G. Modulating skin colour: Role of the thioredoxin and glutathione systems in regulating melanogenesis. Biosci Rep. 2021;41(5):BSR20210427. [CrossRef].
10. Neimkhum W, Anuchapreeda S, Lin W-C, Lue S-C, Lee K-H, Chaiyana W. Effects of Carissa carandas Linn. Fruit, pulp, leaf, and seed on oxidation, inflammation, tyrosinase, matrix metalloproteinase, elastase, and hyaluronidase inhibition. Antioxidants. 2021;10(9):1345. [CrossRef].
11. Ahmed IA, Mikail MA, Zamakshshari N, Abdullah A-SH. Natural anti-aging skincare: role and potential. Biogerontology. 2020;21(3):293–310. [CrossRef].
12. Bazrgaran A, Mahmoodabadi S, Ghasempour A, Shafaie E, Sahebkar A, Eghbali S. Facile bio-genic synthesis of *Astragalus sarcocolla* (Anzaroot) gum extract mediated silver nanoparticles: characterizations, antimicrobial and antioxidant activities. Plant Nano Biol. 2023;6:100052. [CrossRef].
13. Kalam MA, Alam MT, Farooq F. Management of Non-Healing Ulcer with topical application of Marham-i-'Asal-A case study. Int J AYUSH Case Rep. 2021;5(2):78. [CrossRef].
14. Zaheri-Abdevand Z, Badr P. A review of the wound-healing properties of selected plant exudates. J Herb Med. 2023;41:100715. [CrossRef].
15. Nayeem N, Imran M, Asdaq SMB, Rabbani SI, Alanazi FA, Alamri AS, et al. Total phenolic, flavonoid contents, and biological activities of stem extracts of *Astragalus spinosus* (Forssk.) Muschl. grown in Northern Border Province, Saudi Arabia. Saudi J Biol Sci. 2022;29(3):1277–82. [CrossRef].
16. Ababutain IM. Antimicrobial Activity and Phytochemical Screening of *Sarcocolla* Gum Resin. Pak J Biol Sci. 2017;20(11):571–6. [CrossRef].
17. Amiri MS, Joharchi MR, Nadaf M, Nasseh Y. Ethnobotanical knowledge of *Astragalus* spp.: the world's largest genus of vascular plants. Avicenna J Phytomed. 2020;10(2):128. [CrossRef].

18. Pasalar M, Tabatabaei F, Bradley R, Tajadini H, Kamali M, Hasheminasab FS, et al. Mechanistic support of traditional Persian medicine for the treatment of *Acne vulgaris*: a scoping review. J Cosmet Dermatol. 2022;21(6):2338–48. [CrossRef].
19. Li S, Hu X, Liu F, Hu W. Bioactive components and clinical potential of *Astragalus* species. Front Pharmacol. 2025;16:1585697. [CrossRef].
20. Salem MA, El-Shiekh RA, Aborehab NM, Al-Karmalawy AA, Ezzat SM, Alseekh S, et al. Metabolomics driven analysis of *Nigella sativa* seeds identifies the impact of roasting on the chemical composition and immunomodulatory activity. Food Chem. 2023;398:133906. [CrossRef].
21. Kebede BH, Them RL, Mengistu BA. Effects of extraction solvents on phenolic contents, *in vitro* antioxidant, and antimicrobial activities of roselle (*Hibiscus sabdariffa* L.) Calyx. Food Chem Ad. 2025;9:101119. [CrossRef].
22. Elgamal AM, El Raey MA, Gaara A, Abdelfattah MA, Sobeh M. Phytochemical profiling and anti-aging activities of *Euphorbia retusa* extract: *in silico* and *in vitro* studies. Arab J Chem. 2021;14(6):103159. [CrossRef].
23. Sklirou AD, Angelopoulou MT, Argyropoulou A, Chaita E, Boka VI, Cheimonidi C, et al. Phytochemical study and *in vitro* screening focusing on the anti-aging features of various plants of the Greek flora. Antioxidants. 2021;10(8):1206. [CrossRef].
24. Ersoy E, Ozkan EE, Boga M, Yilmaz MA, Mat A. Anti-aging potential and anti-tyrosinase activity of three *Hypericum* species with focus on phytochemical composition by LC–MS/MS. Ind Crops Prod. 2019;141:111735. [CrossRef].
25. Noor F, Rehman A, Ashfaq UA, Saleem MH, Okla MK, Al-Hashimi A, et al. Integrating network pharmacology and molecular docking approaches to decipher the multi-target pharmacological mechanism of *Abrus precatorius* L. acting on diabetes. Pharmaceuticals. 2022;15(4):414. [CrossRef].
26. Gfeller D, Grosdidier A, Wirth M, Daina A, Michielin O, Zoete V. SwissTargetPrediction: a web server for target prediction of bioactive small molecules. Nucleic Acids Res. 2014;42(W1):W32–8. [CrossRef].
27. Szklarczyk D, Santos A, Von Mering C, Jensen LJ, Bork P, Kuhn M. STITCH 5: augmenting protein–chemical interaction networks with tissue and affinity data. Nucleic Acids Res. 2016;44(D1):D380–4. [CrossRef].
28. Safran M, Rosen N, Twik M, BarShir R, Stein TI, Dahary D, et al. The genecards suite. Berlin/Heidelberg, Germany: Springer; 2022. p. 27–56. [CrossRef].
29. UniProt: the universal protein knowledgebase in 2021. Nucleic Acids Res. 2021;49(D1):D480–9. [CrossRef].
30. Alnusaire TS, Qasim S, Al-Sanea MM, Hendawy O, Uttra AM, Ahmed SR. Revealing the underlying mechanism of *Acacia nilotica* against asthma from a systematic perspective: a network pharmacology and molecular docking study. Life. 2023;13(2):411. [CrossRef].
31. Meng EC, Goddard TD, Pettersen EF, Couch GS, Pearson ZJ, Morris JH, et al. UCSF ChimeraX: tools for structure building and analysis. Protein Sci. 2023;32(11):e4792. [CrossRef].
32. Kondapuram SK, Sarvagalla S, Coumar MS. Docking-based virtual screening using PyRx Tool: autophagy target Vps34 as a case study. Amsterdam, The Netherlands: Elsevier; 2021. p. 463–77. [CrossRef].
33. Ghazwani MY, Bakheit AH, Hakami AR, Alkahtani HM, Almehizia AA. Virtual screening and molecular docking studies for discovery of potential RNA-dependent RNA polymerase inhibitors. Crystals. 2021;11(5):471. [CrossRef].
34. Abd-El-Aziz NM, Hifnawy MS, Lotfy RA, Younis IY. LC/MS/MS and GC/MS/MS metabolic profiling of *Leontodon hispidulus*, *in vitro* and *in silico* anticancer activity evaluation targeting hexokinase 2 enzyme. Sci Rep. 2024;14(1):6872. [CrossRef].
35. Mahmoud HN, Elshazly MA, Saad AM, Refahy LA-G, Ghareeb MA, Rizk SA. UPLC-QTOF/MS-assisted chemical profiling of *Daucus carota* leaf extract and evaluation of its antioxidant, antimicrobial and antibiofilm activities: evidence from *in vitro* and *in silico* studies. Egypt J Chem. 2023;66(13):2175–90. [CrossRef].
36. Liu T, Lin S. Comprehensive characterization of the chemical constituents of Lianhua Qingwen capsule by ultra high performance liquid chromatography coupled with Fourier transform ion cyclotron resonance mass spectrometry. Heliyon. 2024;10(6):e27352. [CrossRef].
37. Alves MF, Katchborian-Neto A, Bueno PCP, Carnevale-Neto F, Casoti R, Ferreira MS, et al. LC-MS/DIA-based strategy for comprehensive flavonoid profiling: an Ocotea spp. applicability case. RSC Adv. 2024;14(15):10481–98. [CrossRef].

38. Jiang C, Gates PJ. Systematic characterisation of the fragmentation of flavonoids using high-resolution accurate mass electrospray tandem mass spectrometry. Molecules. 2024;29(22):5246. [CrossRef].
39. Yang C, Sun N, Qin X, Liu Y, Sui M, Zhang Y, et al. Analysis of flavonoid metabolism of compounds in succulent fruits and leaves of three different colors of Rosaceae. Sci Rep. 2024;14(1):4933. [CrossRef].
40. Hamed AR, El-Hawary SS, Ibrahim RM, Abdelmohsen UR, El-Halawany AM. Identification of chemopreventive components from halophytes belonging to Aizoaceae and Cactaceae through LC/MS—bioassay guided approach. J Chromatogr Sci. 2021;59(7):618–26. [CrossRef].
41. Kumar S, Mina PR, Bhatt D, Kumar P, Singh M, Shanker K, et al. Isoliquiritigenin from licorice root: a multi-stage anti-malarial with synergistic impact on multidrug-resistant *P. falciparum*. Pharmacol Res Mod Chin Med. 2024;10:100396. [CrossRef].
42. Wu Z, Singh SK, Lyu R, Pattanaik S, Wang Y, Li Y, et al. Metabolic engineering to enhance the accumulation of bioactive flavonoids licochalcone A and echinatin in *Glycyrrhiza inflata* (Licorice) hairy roots. Front Plant Sci. 2022;13:932594. [CrossRef].
43. Li H, Zhang Y, Dai G, Zhaxi C, Wang Y, Wang S. Identification and quantification of compounds with Angiotensin-converting enzyme inhibitory activity in licorice by UPLC-MS. Food Chem. 2023;429:136962. [CrossRef].
44. Aftab J, Abbas M, Sharif S, Mumtaz A, Zafar K, Ahmad N, et al. LC-MS/MS profiling, antioxidant potential and cytotoxicity evaluation of *Citrus reticulata* Albedo. Nat Prod Commun. 2024;19(8):1934578X241272471. [CrossRef].
45. Divya Priya A, Martin A. UHPLC-MS/MS based comprehensive phenolic profiling, antimicrobial and antioxidant activities of Indian *Rhodomyrtus tomentosa* fruits. Sci Rep. 2025;15(1):945. [CrossRef].
46. Ün RN. LC-MS/MS Analysis and Biological Activities of Methanol Extract from *Sagina apetala* Ard. Celal Bayar Univ J Sci. 2023;19(3):231–5. [CrossRef].
47. Nechita M-A, Pârvu AE, Uifălean A, Iurian S, Olah N-K, Bab TH, et al. LC-MS analysis of the polyphenolic composition and assessment of the antioxidant, anti-Inflammatory and cardioprotective Activities of *Agastache mexicana* and *Agastache scrophulariifolia* extracts. Plants. 2025;14(14):2122. [CrossRef].
48. Dai Y, Dou Z, Zhou R, Luo L, Bian L, Chen Y, et al. Quality evaluation of *Artemisia capillaris* Thunb. Based on qualitative analysis of the HPLC fingerprint and UFLC-Q-TOF-MS/MS combined with quantitative analysis of multicomponents. J Anal Methods Chem. 2021;2021(1):5546446. [CrossRef].
49. Chen J, Sun Y, Li S, Wu H, Guo L, Wei Y, et al. LC-MS/MS method for the simultaneous determination of six phenolic acids in rat plasma and hypoglycemic effects in normal and T2DM rats after oral administration of *Eleutherococcus senticosus* fruits extract. Acta Chromatogr. 2025;37(3):294–306. [CrossRef].
50. Sam-Ang P, Phanumartwiwath A, Liana D, Sureram S, Hongmanee P, Kittakoop P. UHPLC-QQQ-MS and RP-HPLC detection of bioactive alizarin and scopoletin metabolites from *Morinda citrifolia* root extracts and their antitubercular, antibacterial, and antioxidant activities. ACS Omega. 2023;8(32):29615–24. [CrossRef].
51. Sahu R, Kar RK, Sunita P, Bose P, Kumari P, Bharti S, et al. LC-MS characterized methanolic extract of *Zanthoxylum armatum* possess anti-breast cancer activity through Nrf2-Keap1 pathway: An *in-silico*, *in-vitro* and *in-vivo* evaluation. J Ethnopharmacol. 2021;269:113758. [CrossRef].
52. Jakimiuk K, Strawa JW, Granica S, Locatelli M, Tartaglia A, Tomczyk M. Determination of flavonoids in selected *Scleranthus* species and their anti-collagenase and antioxidant potential. Molecules. 2022;27(6):2015. [CrossRef].
53. Păcularu-Burada B, Cîrîc A-I, Begea M. Anti-aging effects of flavonoids from plant extracts. Foods. 2024;13(15):2441. [CrossRef].
54. Abdallah HM, Koshak AE, Farag MA, El Sayed NS, Badr-Eldin SM, Ahmed OA, et al. Taif rose oil ameliorates UVB-induced oxidative damage and skin photoaging in rats via modulation of MAPK and MMP signaling pathways. ACS Omega. 2023;8(37):33943–54. [CrossRef].
55. Shahrivari-Baviloliaei S, Erdogan Orhan I, Abaci Kaplan N, Konopacka A, Waleron K, Plenis A, et al. Characterization of phenolic profile and biological properties of *Astragalus membranaceus* Fisch. ex Bunge commercial samples. Antioxidants. 2024;13(8):993. [CrossRef].
56. Fikry E, Mahdi I, Ortaakarsu AB, Tawfeek N, Ochieng MA, Bakrim WB, et al. Dermato-cosmeceutical properties of *Pseudobombax ellipticum* (Kunth) Dugand: Chemical profiling, *in vitro* and *in silico* studies. Saudi Pharm J. 2023;31(10):101778. [CrossRef]

57. Kiokias S, Proestos C, Oreopoulou V. Phenolic acids of plant origin—A review on their antioxidant activity *in vitro* (o/w emulsion systems) along with their *in vivo* health biochemical properties. Foods. 2020;9(4):534. [CrossRef].
58. Shen N, Wang T, Gan Q, Liu S, Wang L, Jin B. Plant flavonoids: Classification, distribution, biosynthesis, and antioxidant activity. Food Chem. 2022;383:132531. [CrossRef].
59. Merecz-Sadowska A, Sitarek P, Kucharska E, Kowalczyk T, Zajdel K, Cegliński T, et al. Antioxidant properties of plant-derived phenolic compounds and their effect on skin fibroblast cells. Antioxidants. 2021;10(5):726. [CrossRef].
60. Kurt-Celep İ, Zengin G, Sinan KI, Ak G, Elbasan F, Yıldıztugay E, et al. Comprehensive evaluation of two *Astragalus* species (*A. campylosema* and *A. hirsutus*) based on biological and toxicological properties and chemical profiling. Food Chem Toxicol. 2021;154:112330. [CrossRef].
61. Gendrisch F, Esser PR, Schempp CM, Wölfle U. Luteolin as a modulator of skin aging and inflammation. Biofactors. 2021;47(2):170–80. [CrossRef].
62. Jesus EGD, Souza FFD, Andrade JV, Andrade e Silva ML, Cunha WR, Ramos RC, et al. *In silico* and *in vitro* elastase inhibition assessment of rosmarinic acid from *Rosmarinus officinalis* Linn. Nat Prod Res. 2024;38(5):879–84. [CrossRef].
63. Allemailem KS, Almatroudi A, Alharbi HOA, AlSuhaymi N, Alsugoor MH, Aldakheel FM, et al. Apigenin: a bioflavonoid with a promising role in disease prevention and treatment. Biomedicines. 2024;12(6):1353. [CrossRef].
64. Al-Ghanayem AA. *In vitro* anti-acne activity of *Teucrium oliverianum* methanolic extract against Cutibacterium acnes. Front Pharmacol. 2024;15:1388625. [CrossRef].
65. Khojah H, Ahmed SR, Alharbi SY, AlSabeelah KK, Alrayyes HY, Almusayyab KB, et al. Skin anti-aging potential of *Launaea procumbens* extract: Antioxidant and enzyme inhibition activities supported by ADMET and molecular docking studies. Saudi Pharm J. 2024;32(7):102107. [CrossRef].
66. Noor F, Tahir ul Qamar M, Ashfaq UA, Albutti A, Alwashmi AS, Aljasir MA. Network pharmacology approach for medicinal plants: review and assessment. Pharmaceuticals. 2022;15(5):572. [CrossRef].
67. Ke D, Zhang H, Tian LM, Han M, Zhang C, Tian DZ, et al. A network pharmacology-based study of the potential targets and mechanisms of action of Qibao Meiran Dan in delaying skin aging. J Cosmet Dermatol. 2022;21(10):4956–64. [CrossRef].
68. Haoran W, Jinyv Z, Shikui C, Jingwei L. Research on the mechanisms of plant bioactive metabolites in anti-skin aging and future development prospects. Front Pharmacol. 2025;16:1673075. [CrossRef].
69. Li Y, Lei D, Swindell WR, Xia W, Weng S, Fu J, et al. Age-associated increase in skin fibroblast–derived prostaglandin E2 contributes to reduced collagen levels in elderly human skin. J Investig Dermatol. 2015;135(9):2181–8. [CrossRef].
70. Nanba D, Toki F, Asakawa K, Matsumura H, Shiraishi K, Sayama K, et al. EGFR-mediated epidermal stem cell motility drives skin regeneration through COL17A1 proteolysis. J Cell Biol. 2021;220(11):e202012073. [CrossRef].
71. Guan G, Chen Y, Dong Y. Unraveling the AMPK-SIRT1-FOXO pathway: the in-depth analysis and breakthrough prospects of oxidative stress-induced diseases. Antioxidants. 2025;14(1):70. [CrossRef].
72. Frantz MC, Rozot R, Marrot L. NRF2 in dermo-cosmetic: From scientific knowledge to skin care products. Biofactors. 2023;49(1):32–61. [CrossRef].
73. Huang H, Han J, Liu Y, Zhang Q, Zhou Y, Zheng S, et al. Exploring the molecular mechanism of apigenin in treating bronchiectasis based on network pharmacology and molecular docking. Sci Rep. 2025;15(1):39161. [CrossRef].
74. Ouyang Y, Rong Y, Wang Y, Guo Y, Shan L, Yu X, et al. A systematic study of the mechanism of acacetin against sepsis based on network pharmacology and experimental validation. Front Pharmacol. 2021;12:683645. [CrossRef].